*Proc. Natl. Acad. Sci. USA*
Vol. 91, pp. 4534–4538, May 1994
Biochemistry

# Spontaneous generation of a biradical species of neocarzinostatin chromophore: Role in DNA bulge-specific cleavage

(enediyne/Bergman rearrangement/mechanism of activation/spirolactone/stereoselective Michael addition)

OTTO D. HENSENS*†, DER-HANG CHIN‡, ADONIS STASSINOPOULOS‡, DEBORAH L. ZINK*, LIZZY S. KAPPEN‡, AND IRVING H. GOLDBERG†‡

*Natural Products Chemistry Department, Merck Research Laboratories, Rahway, NJ 07065; and ‡Department of Biological Chemistry and Molecular Pharmacology, Harvard Medical School, Boston, MA 02115

*Communicated by JoAnne Stubbe, February 14, 1994 (received for review December 1, 1993)*

ABSTRACT **Detailed structure determination of the major and minor base-catalyzed degradation products of the chromophore of the enediyne anticancer antibiotic neocarzinostatin in the absence of DNA demonstrates that the enolate Michael addition reaction leading to a spirolactone cumulene intermediate is a spontaneous, stereoselective process. The implications of these findings for the mechanism of the thiol-independent, site-specific cleavage by the so-generated radical species of the drug at a DNA bulge are described.**

The chromophore of the enediyne anticancer antibiotic neocarzinostatin (NCS-Chrom) induces highly efficient site-specific cleavage at the 3′ side of a DNA bulge in the absence of thiol activator in a reaction involving general base catalysis (1, 2). By contrast, thiol is required in the nucleophilic activation of the drug to its biradical form for cleavage of duplex DNA. Only a reaction mixture containing bulged DNA, but lacking thiol, generates a new product **3** of NCS-Chrom (Fig. 1), whose unusual structure was recently reported (3). Based on its structure, it was proposed that the formation of **3** involves the naphthoate ester moiety as both a nucleophile and radical quencher as depicted in Fig. 1. Specifically, the mechanism leading to the biradical **1d** can be envisaged as proceeding by an unusual *5-exo-trig* intramolecular Michael addition (4, 5) involving the enolate **1b**, which is a resonance form of the naphtholate anion **1a** of NCS-Chrom ($pK_a \approx 8.5$). This is consistent with general base catalysis of the DNA cleavage reaction, having a pH optimum of ≈9.0 (1, 2). Epoxide ring opening, in a concerted reaction with the Michael addition, leads to the cumulene intermediate **1c**, which then undergoes a Bergman-type rearrangement to the 2,6-biradical **1d** (6–8) and eventuates in **3**.

In a drug-induced cleavage reaction **3** became labeled with $^3H$ abstracted from the C-5′ position of the target nucleotide, whereas two other unidentified fluorescent products were unlabeled (1). The latter two materials were also found in a reaction mixture not containing any DNA or with DNA lacking the bulged structure. Since **3** was formed only in the presence of bulged DNA, it appears that DNA played a critical role, presumably via some conformational mechanism, in effecting the intramolecular reaction of step 2 and/or step 4 (Fig. 1). Thus, it was important to determine the structures of the two products made in the absence of bulged DNA, and in smaller amounts in its presence, in order to assess whether these spontaneous degradation products and **3** shared similar steps in their formation.

Based on the structure of the two main spontaneous products reported here, it is now clear that steps 1–3 are not DNA dependent and that bulged DNA, acting as an effector molecule, is required for step 4. It is also shown that step 2, involving spirolactone formation, is a stereoselective process. Furthermore, the data implicate the cumulene as the key intermediate that recognizes the DNA bulged structure. Based on these and other findings, we can now propose possible mechanisms of formation of the unusual DNA cleaving species and the role of DNA conformation in its generation.

## MATERIALS AND METHODS

**Instrumentation.** $^1H$ and $^{13}C$ NMR data were obtained on a Varian Unity 500 spectrometer in $C^2H_3O^2H$ ($^2H$, 99.96%) at 25°C using 3-mm indirect detection and dual $^1H/^{13}C$ microprobes, respectively (Nalorac Cryogenics, Martinez, CA). $^1H$-detected experiments [$^1H$-detected heteronuclear multiple-quantum coherence (HMQC), heteronuclear multiple bond connectivity (HMBC), and nuclear Overhauser enhancement spectroscopy (NOESY)] were carried out with presaturation of either the solvent or residual $HO^2H$ peak. HMBC experiments were optimized for 4 and 7 Hz. A mixing time of 0.5 sec was used in the NOESY experiments.

Fast atom bombardment mass spectroscopy (FAB-MS) data were acquired on a JEOL HX110 mass spectrometer using glycerol as matrix. The exact mass measurements were made at high resolution with Ultramark 1960 (Fomblin) as the reference compound. Linked scan daughter analysis was performed on the same instrument. Confirmation of molecular weights was obtained by electrospray ionization (ESI)-MS on a Finnigan TSQ700 instrument.

**Isolation Procedure.** Isolation of the major (**2a**; 55–60%; retention time, 63 min) and minor (**2b**; 10–15%; retention time, 50 min) peaks on reverse-phase HPLC ($C_{18}$ column) was similar to that previously described (1). After incubation of NCS-Chrom (50–80 μM) in 7.5 mM Tris·HCl, pH ≈8.5/10% MeOH in the absence of DNA (0°C; 0.5 hr), the reaction mixture was lyophilized, and the dried sample was redissolved in 100 mM ammonium acetate (pH 4) for HPLC purification. **2a** and **2b** were isolated and subjected to repeated HPLC on a 4.6 × 250 mm $C_{18}$ column (Ultrasphere; Beckman) using a linear gradient of 35–55% solvent B/solvent A over a 1-hr period [solvent A, aqueous 5 mM ammonium acetate (pH 4); solvent B, methanolic 5 mM ammonium acetate (pH 4); flow rate, 1 ml/min].

Due to the limited amounts of materials isolated, the absolute extinction coefficients for **2a** and **2b** were not

The publication costs of this article were defrayed in part by page charge payment. This article must therefore be hereby marked "*advertisement*" in accordance with 18 U.S.C. §1734 solely to indicate this fact.

Abbreviations: NCS-Chrom, chromophore of neocarzinostatin; NOE, nuclear Overhauser effect; NOESY, nuclear Overhauser enhancement spectroscopy; HMQC, $^1H$-detected heteronuclear multiple-quantum coherence; HMBC, heteronuclear multiple bond connectivity; FAB-MS, fast atom bombardment mass spectrometry; ESI-MS, electrospray ionization mass spectrometry.

†To whom reprint requests should be addressed.

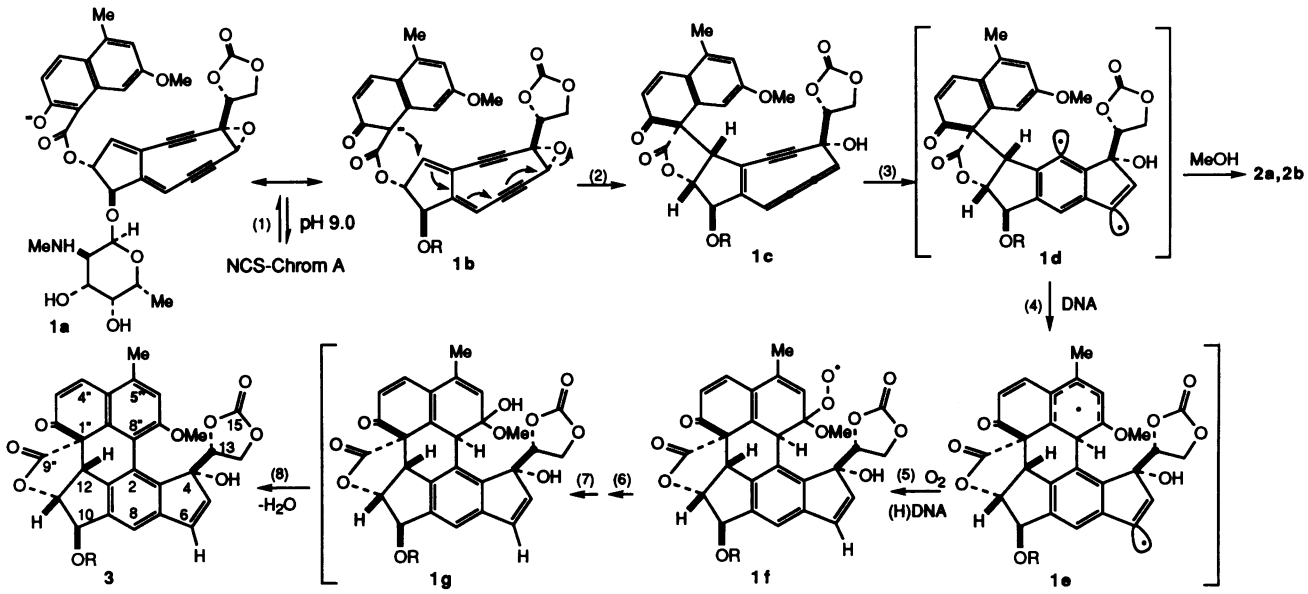


FIG. 1. Proposed thiol-independent mechanism of action of NCS-Chrom.

determined with any degree of accuracy, but the ratio of the extinction coefficients at 254 nm $\varepsilon_{2b}/\varepsilon_{2a}$ is ≈2.5. A minor fluorescent peak eluting with a retention time of 70 min was not further characterized. It was present in various amounts (5–30%) and was composed of at least three components, two of which are decomposition products of **2a** and **2b** under alkaline conditions and elevated temperatures.

**Major Component** (2a). FAB-MS: $C_{35}H_{35}NO_{12}$ found $m/z$ 662.2269; calculated $m/z$ 662.2238 $[M + H]^+$. Linked scan daughter analysis of $[M + H]^+$: $m/z$ 503, 432, 214, 160. ESI-MS $m/z$ 662 $[M + H]^+$. UV/visible (MeOH): $\lambda_{max}$, ≈220, ≈255, ≈375 nm. Fluorescence excitation (MeOH): $\lambda_{max}$, ≈235 (sh), 270, ≈390 nm. Fluorescence emission (MeOH): $\lambda_{max}$, 500 nm. $^1H$ and $^{13}C$ NMR in $C^2H_3O^2H$ (see Table 1).

**Minor Component** (2b). FAB-MS: $C_{36}H_{37}NO_{13}$ found $m/z$ 692.2358; calculated $m/z$ 692.2343 $[M + H]^+$. Linked scan daughter analysis of $[M + H]^+$: $m/z$ 605, 462, 214, 160. ESI-MS $m/z$ 692 $[M + H]^+$. UV/visible (MeOH): $\lambda_{max}$, ≈225, ≈255, ≈375 nm. Fluorescence excitation (MeOH): $\lambda_{max}$, ≈240 (sh), 270, ≈390 nm. Fluorescence emission (MeOH): $\lambda_{max}$, 490 nm. $^1H$ and $^{13}C$ NMR in $C^2H_3O^2H$ (see Table 1).

## RESULTS AND DISCUSSION

Spectroscopic data of the major product (≈500 μg), isolated after incubation of NCS-Chrom in 50 mM Tris·HCl (pH ≈ 8.5) in the absence of DNA, suggested a rearranged structure 2 mass units higher than NCS-Chrom or **3** (Fig. 1). The carbon count of 35 was confirmed by the $^{13}C$ NMR spectrum. The two additional $^1H$ NMR resonances in the δ 5.0–8.0 region compared to **3** (3) were readily assigned to the protons at the C2 and C8″ positions (Table 1) on the basis of $^1H$-$^1H$ correlated spectroscopy (COSY), delayed COSY, and phase-sensitive NOESY experiments. The data also allowed unequivocal assignment of all protons around the periphery of the indacenyl (H5–H12) and naphthoate (H3″–H8″) ring skeletons. Proceeding similarly as for **3** (3), HMQC data allowed assignment of all protonated carbons, whereas HMBC experiments provided 2- and 3-bond $^1H$-$^{13}C$ correlations (Table 1) consistent with the proposed structure **2a** (Fig. 2).

Similarly, **2b** (Fig. 2) is proposed for the structure of the minor component, which differs from **2a** by the elements $CH_2O$ as determined by high-resolution FAB-MS. Because of limited quantities of sample (≈100 μg), all carbon resonances with the exception of the lactone carbonyl were indirectly detected via the HMQC and HMBC $^1H$-detected experiments. The absence of H2 in the $^1H$ NMR spectrum and strong HMBC correlations from the methylenehydroxy protons (δ 3.80 and 4.18) into C1, C2, and C3 readily define the position of the $CH_2OH$ group at C2. FAB-MS linked scan daughter analyses of the precursor M + H ions for **2a** and **2b** support the structure proposals (Fig. 2). In particular, loss of the naphthoate moiety from both components can be readily envisaged as shown.

The yield of **2b** is critically dependent on the proportion of methanol in the buffered solution, which suggests that the C-6 radical abstracts a hydrogen atom from methanol in the solvent to form a hydroxy methylene radical, which then recombines with the C-2 radical to form **2b**. **2b** is also not formed when methanol is substituted by another alcohol (ethanol, propanol). The formation of **3** and **2b** involves an intramolecular and an intermolecular radical quenching reaction of an enediyne natural product, respectively, via carbon-carbon bond formation.

The stereochemistry at C1″ and C12 of **2a** was determined as follows. The trans arrangement of the substituents at C10 and C11 and the cis arrangement at C11 and C12 were evident from the proton-proton coupling constants ($^3J_{10,11} < 1.0$, $^3J_{11,12} = 5.6$ Hz) and strong NOE between H11 and H12 as observed for **3** (3), which therefore defines the absolute stereochemistry at these centers as 10*R*, 11*R*, and 12*S*. The *S* configuration at C1″ as in **3** (3) was deduced on the basis of conformational analysis of both 1″*S* and 1″*R* structures taking into account the low-field resonance position of H12 (δ 4.63) and the >2 ppm shielded positions of H2 (δ 5.86) and H8″ (δ 5.67) (8). One of the two likely flattened half-chair conformations for ring A of the naphthoate moiety, as depicted in Fig. 3 (see **2a**), readily accounts for these observations where H2 falls above ring B of the naphthoate ring and is shielded by its ring currents. H8″ falls in the shielding cone of the lactone carbonyl group, and H12 falls outside and in the deshielding region of this cone. Of the four likely conformations examined (two half-chair conformations for both 1″*S* and 1″*R* forms), that depicted for **2a** in Fig. 3 places H12 and H3″ in closest proximity, which therefore accounts for the only NOE (H3″ → H12) observed between the naphthoate

Table 1. $^1H$ and $^{13}C$ NMR data for **2a** and **2b** in $C^2H_3O^2H$

| | **2a** | | | **2b** | |
|---|---|---|---|---|---|
| No. | $^{13}C$, ppm | $^1H$, ppm (m, *J* in Hz) | HMBC (4 and 7 Hz) | $^{13}C$, ppm | $^1H$, ppm (m, *J* in Hz) |
| 1 | 138.7 | | | 139.2 | |
| 2 | 124.9 | 5.86 s | C3, C4, C7, C9, C12 | 136.9 | |
| 3 | 148.4 | | | 145.7 | |
| 4 | 84.2 | | | 87.2 | |
| 5 | 138.0 | 6.22 d, 5.9 | C3, C4, C6, C7 | 137.2 | 6.29 d, 5.8 |
| 6 | 135.4 | 6.86 d, 5.9 | C3, C4, C5, C7 | 135.5 | 6.95 d, 5.8 |
| 7 | 145.1 | | | 146.8 | |
| 8 | 120.7 | 7.35 s | C1, C3, C6, C10 | 119.8 | 7.38 s |
| 9 | 141.9 | | | 143.2 | |
| 10 | 83.9 | 5.42 bs | C1, C8, C9, C11, C12, C1′ | 85.8 | ≈5.61 bs* |
| 11 | 85.9 | 5.35 bd, 5.6 | C1, C9, C10 | 88.4 | ≈5.63 bs† |
| 12 | 56.2 | 4.63 bd, 5.6 | C1, C2, C9, C1″, C2″, C8a″, C9″ | 57.5 | 5.08 bd, 7.7‡ |
| 13 | 81.1 | 4.40 dd, 4.9, 8.4 | C4, C14, C15 | 81.9 | 5.27 dd, 6.6, 8.4 |
| 14a | 67.1 | 4.27 dd, 4.9, 7.8 | C4, C13, C15 | 67.0 | 3.21 dd, 6.6, 8.5 |
| 14b | | 4.36 t, ≈8.2 | C4, C15 | | 4.10 t, 8.5 |
| 15 | 157.1 | | | 157.1 | |
| 16a | — | — | | 58.3 | 3.80 d, 12.2 |
| 16b | | | | | 4.18 d, 12.2 |
| 1′ | 96.0 | 5.32 bm | C10, C3′ | 95.8 | 5.52 bs§ |
| 2′ | 59.6 | 3.19 bm | | 59.2 | ≈3.30 m |
| 2′-NHMe | 33.3 | 2.65 bs | C2′ | 32.6 | 2.72 bs |
| 3′ | 69.2 | 3.74 bd, ≈9.5 | | 68.8 | 3.87 m |
| 4′ | 72.5 | 3.61 bs | | 72.3 | 3.71 bs |
| 5′ | 68.7 | 3.85 bq, 6.6 | C4′, 5′-Me | 68.3 | 4.06 bq, 6.5 |
| 5′-Me | 16.5 | 1.22 d, 6.2 | C4′, C5′ | 16.1 | 1.32 d, 6.5 |
| 1″ | 68.7 | | | 65.3 | |
| 2″ | 199.2 | | | 199.0 | |
| 3″ | 119.3 | 6.10 d, 10.1 | C1″, C4a″ | 120.6 | 6.19 d, 10.1 |
| 4″ | 145.5 | 8.09 d, 10.1 | C2″, C5″, C8a″ | 145.9 | 8.07 d, 10.1 |
| 4a″ | 122.7 | | | 122.8 | |
| 5″ | 142.0 | | | 141.3 | |
| 5″-Me | 19.4 | 2.58 s | C4a″, C5″, C6″ | 19.1 | 2.45 s |
| 6″ | 116.4 | 6.82 dq, 2.5, 0.7 | C4a″, 5″-Me, C8″ | 117.6 | 6.66 bd, 2.4 |
| 7″ | 162.0 | | | 161.9 | |
| 7″-OMe | 55.8 | 3.57 s | C7″ | 55.3 | 3.37 s |
| 8″ | 118.3 | 5.67 dq, 2.5, 0.6 | C1″, C4a″, C6″, C7″ | 114.5 | 5.41 d, 2.4 |
| 8a″ | 138.5 | | | 140.5 | |
| 9″ | 175.7 | | | | |

$^{13}C$ data for **2a** were at 125 MHz; $C^2H_3O^2H$ signal at 49.0 ppm. $^1H$ data for **2a** and **2b** were at 500 MHz; $C^2H_3O^2H$ signal at δ 3.30. $^{13}C$ data for **2b** were indirectly $^1H$-detected via HMQC and HMBC. Sharpened signals resulted when spiked with $C^2H_3COO^2H$ for the following resonances: *, 5.66 bd, ≈1.5¶; †, 5.63 dd, 1.9, 8.2¶; ‡, 5.08 d, 8.2¶; §, 5.60 d, 3.4. ¶, The H10, H11, H12 spin system forms a tight ABX pattern; hence, the splittings are not the actual coupling constants.

and indacenyl moieties.§ The minor product **2b** was similarly shown to have the 1″*S* configuration. However, ring A of the naphthoate moiety now adopts the alternative half-chair conformation (see **2b**, Fig. 3) as suggested by the significant NOE between H8″ and H10. H12 (δ 5.08) is deshielded relative to its chemical shift position in **2a** as it now falls in the deshielding plane containing the lactone carbonyl group. On the other hand, H8″ (δ 5.41) falls below the indacene ring system and is therefore shielded by its ring currents. Steric interference between the newly introduced hydroxymethylene moiety at C2 and ring A of the naphthoate in the conformation adopted by **2a** forces the molecule to assume this more stable, alternative conformation (**2b**, Fig. 3). Restricted rotation of the cyclic carbonate ring about the C4-C13 bond as a result of nonbonded interaction between the ring and the hydroxymethylene group, as evidenced by the strong NOEs between H13 (δ 5.27) and H14a (δ 3.21) with one of the $CH_2OH$ protons (δ 4.18), appears to be responsible for the differential shielding of the H13/H14 resonances in **2a** and **2b** (Table 1). This is even more apparent in **3**, where a strong NOE was observed between H13 and the C7″-OMe, and the chemical shift positions for H13 (δ 6.15), H14a (δ 3.64), and H14b (δ 4.40) are even more dispersed (3).

Recent neocarzinostatin model studies (4) suggest that the kinetically controlled formation of the spirolactone cumulene

§Moreover, no NOE was observed between H12 and H8″ as expected for the 12*S*, 1″*R* structure on the basis of the NOE findings by Lamothe and Fuchs (4) for the spirolactone (denoted **35**) having the opposite relative stereochemistry at the positions equivalent to that of **2a**. This assumes that the predominant half-chair conformation of ring A of the naphthoate moiety in both molecules is similar.

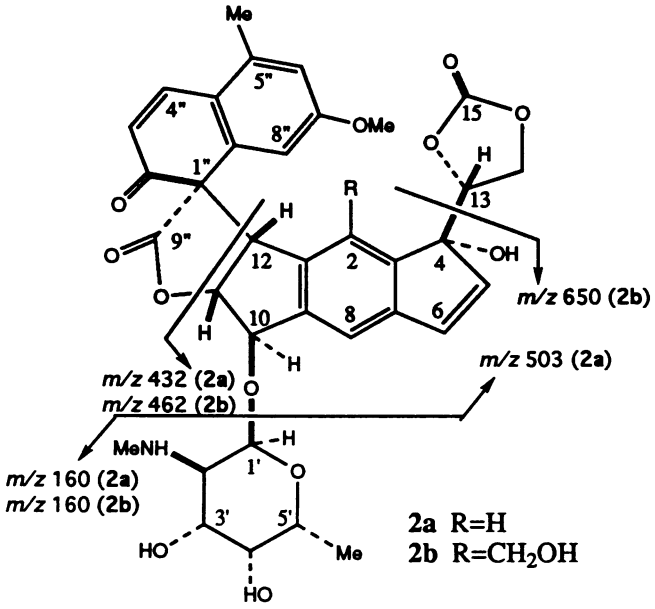


FIG. 2. Structures and FAB-MS linked scan daughter analysis of **2a** (R = H) and **2b** (R = $CH_2OH$) showing the M + H precursor ions.

intermediate **1c** (step 2) may be a spontaneous process (Fig. 1). The formation of **2a** in the absence of DNA is consistent with this proposal. The stereoselectivity of the reaction has similar precedence in the work of Lamothe and Fuchs (4) and in intramolecular Michael additions in general (5) and points to some structural organization in the reaction pathway to **2a**. One such proposal is shown in **1a**, where the chromophore folds in a manner so as to allow optimal $\pi$-orbital interaction

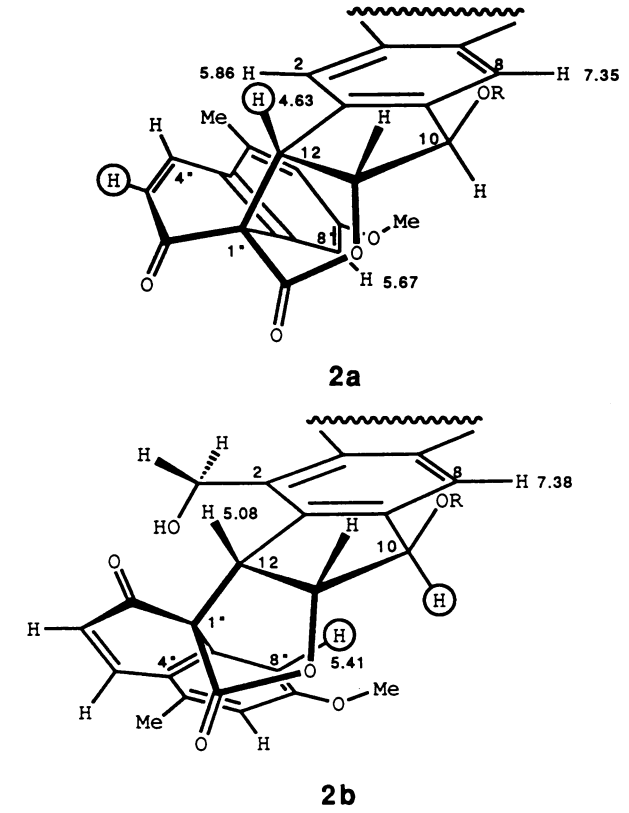


FIG. 3. Proposed conformations for **2a** and **2b** depicting alternative, flattened half-chair conformations for ring A of the naphthoate moiety. NOEs were observed between the circled protons.

between the naphtholate and bicyclo[7.3.0]dodecadienyne ring skeletons. It is noteworthy that the remarkable stereoselectivity is preserved under widely differing reaction conditions from the anhydrous conditions used for the neocarzinostatin model studies (4) to the buffered aqueous conditions used in this work for the chromophore itself.

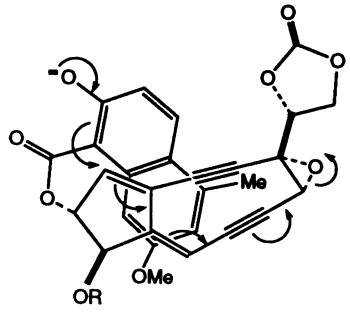


Structure **1a**

In the absence of bulged DNA, **3** was not formed to any significant extent (1). Furthermore, **3** contained $^3H$ abstracted from C5′ of the target nucleotide of bulged DNA, whereas no label was found in either **2a** or **2b**, whose yields were reduced compared to the spontaneous reaction (1). These results suggest that in the presence of bulged DNA cumulene **1c** exists in equilibrium between bound and free forms, which lead to **3** and to **2a** and **2b**, respectively, via **1d**. The DNA bulge presumably alters the conformation of bound **1d** to enable its conversion to **1e** (step 4, Fig. 1). It is not possible to distinguish whether H abstraction from C5′ of deoxyribose occurs before (by bound **1d**) or after **1e** formation, although it is likely that the intramolecular formation of a bond between C2 and C8″ would occur first. The DNA cleavage sites for the spontaneously activated and thiol-activated species of NCS-Chrom are distinctly different (1, 2), implicating the respective cumulene intermediates as the species that search for the favored DNA binding site. Consistent with this proposal is the finding of a relatively long half-life for the thiol-generated cumulene intermediate (9). Such a possibility was first suggested by Townsend for the thiol-dependent reaction (10).

Thus, it is conceivable that after DNA bulge-specific binding of the cumulene **1c** and cycloaromatization to the $\sigma,\sigma$-biradical **1d**, the species undergoes a further intramolecular radical cyclization reaction to the $\sigma,\pi$-biradical **1e**, characterized by the localized $\sigma$-radical at C6 and delocalized cyclohexadienyl $\pi$-radical (11, 12). Subsequent oxidation of the latter in the presence of oxygen with loss of the C8″-H may be envisaged to occur simultaneously with specific hydrogen abstraction from C5′ of deoxyribose by C6 to form **3**. The C5′ radical is further converted to the hydroperoxide (via the peroxy radical), which would be expected to undergo spontaneous degradation to the aldehyde to generate the DNA strand break. Even though **1e** is represented with a delocalized cyclohexadienyl $\pi$-radical, the bond formation occurs at C7″, adjacent to the methoxy group.

One possible route to **3** therefore is depicted in Fig. 1 via the C7″-hydroperoxide, involving elimination of water across the C7″-C8″ bond in the final step (13). Alternatively, by analogy with Dorfman's mechanism (13, 14), stereospecific abstraction of the C8″-H by the peroxy radical at C7″ with direct elimination of the hydroperoxy radical (H-O-O·) from **1f** should not be discounted. Formation of the monofunctional species **1e** with only one $\sigma$-radical center (at C6) for potential hydrogen abstraction may account for its remarkable specificity, compared to the thiol-dependent reaction, in producing only a single-strand break at the target site.

A related, intermolecular counterpart to the latter mechanism may be entertained. Depending on the overall kinetics and the geometry of the bulged DNA–NCS-Chrom intermediate complex, it is (remotely) conceivable that one-electron oxidation occurs not by internal abstraction of the C8″-H by the peroxy radical at C7″ (**1f** → **3**) but by the analogous direct intervention of the C5′ deoxyribose peroxy radical (**1e** → **3**). In the same vein, it is also possible that the presumed drug–DNA adduct formed quantitatively in the absence of oxygen (1, 2) results from recombination of the C5′ deoxyribosyl and cyclohexadienyl radicals.

In summary, while it is possible to propose different mechanistic scenarios leading from **1d** to **3**, it is clear that DNA conformation plays a role in step 4 (Fig. 1) of this sequence, the conversion of **1d** to **1e**, which does not occur in the spontaneous reaction. Presumably, the DNA bulged structure induces a conformational change in **1d** so that the radical generated at C2 is quenched intramolecularly by ring B of the naphthoate, forming a bond between C8″ and C2. In the absence of bulged DNA the radical center at C2 is, instead, quenched intermolecularly by solvent.

We wish to acknowledge very useful discussions on the stereoselectivity of the Michael addition reaction with Dr. Steve Pitzenberger. This work was supported by National Institutes of Health Grant CA44257.

1. Kappen, L. S. & Goldberg, I. H. (1993) *Science* **261,** 1319–1321.
2. Kappen, L. S. & Goldberg, I. H. (1993) *Biochemistry* **32,** 13138–13145.
3. Hensens, O. D., Helms, G. L., Zink, D. L., Chin, D.-H., Kappen, L. S. & Goldberg, I. H. (1993) *J. Am. Chem. Soc.* **115,** 11030–11031.
4. Lamothe, M. & Fuchs, P. L. (1993) *J. Am. Chem. Soc.* **115,** 4483–4496.
5. Oare, D. A. & Heathcock, C. H. (1989) in *Topics in Stereochemistry*, eds. Eliel, E. L. & Wilen, S. H. (Wiley, New York), Vol. 19, pp. 355–374.
6. Myers, A. G. (1987) *Tetrahedron Lett.* **28,** 4493–4496.
7. Myers, A. G., Proteau, P. J. & Handel, T. M. (1988) *J. Am. Chem. Soc.* **110,** 7212–7214.
8. Hensens, O. D. & Goldberg, I. H. (1989) *J. Antibiot.* **42,** 761–768.
9. Myers, A. G. & Proteau, P. J. (1989) *J. Am. Chem. Soc.* **111,** 1146–1147.
10. De Voss, J. J., Hangeland, J. J. & Townsend, C. A. (1990) *J. Am. Chem. Soc.* **112,** 4554–4556.
11. Beckwith, A. L. J. & Ingold, K. U. (1980) in *Rearrangements in Ground and Excited States*, ed. de Mayo, P. (Academic, New York), Vol. 1, pp. 209–215.
12. Scheuplein, S. W., Machinek, R., Suffert, J. & Bruckner, R. (1993) *Tetrahedron Lett.* **34,** 6549–6552.
13. Narita, N. & Tezuka, T. (1982) *J. Am. Chem. Soc.* **104,** 7316–7318.
14. Dorfman, L. M., Taub, I. A. & Buhler, R. E. (1962) *J. Chem. Phys.* **36,** 3051–3061.